Advances in Biometrics

Nalini K. Ratha • Venu Govindaraju
Editors

Advances in Biometrics

Sensors, Algorithms and Systems

Springer

Nalini K. Ratha, BTech, MTech, PhD
IBM Thomas J. Watson Research Center
Hawthorne, New York, USA

Venu Govindaraju, BTech, MS, PhD
Department of Computer Science and Engineering
University of Buffalo, New York, USA

ISBN: 978-1-84628-920-0 e-ISBN: 978-1-84628-921-7

British Library Cataloguing in Publication Data
A catalogue record for this book is available from the British Library

Library of Congress Control Number: 2007929188

Printed on acid-free paper

9 8 7 6 5 4 3 2 1

Springer Science+Business Media
springer.com

Preface

Overview and Goals

Recognizing people based on their physiological or behavioral characteristics is the main focus of the science of biometrics. With the ever-increasing need for secure and reliable human identification methods in a highly security-conscious society spurred by recent events around the world, biometrics has surged from an interesting application of pattern-recognition techniques to a vibrant mainstream research topic over the last decade. The exponential growth of research in this area focuses on many challenging research problems including evaluating new biometrics techniques, significantly improving accuracy in many existing biometrics, new sensing techniques, and large-scale system design issues. Biometrics technology relies on advances in many allied areas including pattern recognition, computer vision, signal/image processing, statistics, electrical engineering, computer science, and machine learning. Several books, conferences, and special issues of journals have been published and many are in the active pipeline covering these advanced research topics.

Most of the published work assumes the biometric signal has been reliably acquired by the sensors and the task is one of controlling false match and false rejection rates. Thus, the focus and thrust of many researchers have been on pattern recognition and machine-learning algorithms in recognizing biometrics signals. However, the emphasis on the sensors themselves, which are critical in capturing high-quality signals, has been largely missing from the research discourse. We have endeavored to remedy this by including several chapters relating to the sensors for the various biometric modalities. This is perhaps the first book to provide a comprehensive treatment of the topic. Although covering the sensing aspect of biometrics at length, we are also equally excited about new algorithmic advances fundamentally changing the course for some of the leading and popular biometrics modalities as well as new modalities that may hold a new future. There has also been interest at the systems level both from a human factors point of view and the perspective of networking, databases, privacy, and antispoofing. Our goal in designing this book has been primarily based on covering many recent advances made in these three key areas: sensors, algorithms, and systems.

Organization and Features

The chapters in this book have been authored by the leading authorities in the field making this book a unique blueprint of the advances being made on all frontiers of biometrics with coverage of the entire gamut of topics including data acquisition, pattern-matching algorithms, and issues such as standards, security, networks, and databases that have an impact at the system level. Accordingly, the book has been organized under three roughly clustered parts: Part I pertains to sensors, Part II is about advances in biometric matching algorithms, and Part III deals with issues at the systems level. Chapters within any one cluster are self-explanatory and do not depend on prior chapters.

We have emphasized the advances and cutting-edge technologies in each of the parts with the understanding that readers have other options for looking up matching algorithms for commonly used modalities such as fingerprint and face recognition. Our focus has been on the newer modalities, be it the use of infrared imaging for measuring the distinguishing features in vascular structures, multispectral imaging to ensure liveness, or iris on the move for unobtrusive identification in surveillance scenarios. With respect to fingerprints, we have devoted chapters in Part I to touchless image capture, ultrasonic imaging, and swipe methods.

Part II is divided roughly equally between behavioral (handwriting, voice) and physical biometrics (face, iris) with an additional chapter on a strikingly novel modality in headprint biometrics.

Readers will also find the inclusion of the chapter on standards in Part III to be an extremely convenient reference.

Target Audience

The primary intended audience for this book is the research community both from industry and academia as reflected by the authorship of the chapters where we have roughly equal participation from both. The insight provided by the industry chapters is invaluable as it provides the perspective of actual working systems. We anticipate the book to be a ready reference on the state of the art in biometric research.

The secondary audience is graduate students taking an advanced research topics course on their way to a doctoral dissertation. This will be well suited for students specializing in biometrics, image processing, and machine learning as it can provide ideal application testbeds to test their algorithms. The benchmarks provided for several modalities in Part II should prove to be useful as well.

Acknowledgments

We are extremely thankful to all the chapter authors who have contributed to make this book a unique resource for all researchers. The 24 chapters are the combined effort of 53 authors. We have truly enjoyed interacting with them at all stages of book preparation: concept, drafts, proofs, and finalization. We would also like to thank Achint Thomas for helping with the FTP submissions of the manuscripts and proofreading. Last, but not least, we are grateful to Springer for constantly driving us for timely completion of the tasks on our end.

Hawthorne, New York — Nalini K. Ratha
Buffalo, New York — Venu Govindaraju
April 2007

Contents

Part III Systems

Contributors

David Ackerman
Sarnoff Corporation,
Princeton, NJ 08543-5300, USA,
dackerman@sarnoff.com

Gaurav Aggarwal
Center for Automation Research and
Department of Computer Science,
University of Maryland,
College Park, MD 20742, USA,
gaurav@cs.umd.edu

Hrishikesh Aradhye
SRI International,
333 Ravenswood Avenue,
Menlo Park, CA 94025, USA,
hrishikesh.aradhye@sri.com

James Bergen
Sarnoff Corporation,
Princeton, NJ 08543-5300, USA,
jbergen@sarnoff.com

Christer Bergman
Precise Biometrics AB,
Lund, Sweden,
christer@novexus.com

Robert Bolles
SRI International,
333 Ravenswood Avenue,
Menlo Park, CA 94025, USA,
robert.bolles@sri.com

Terrance E. Boult
Department of Computer Science,
University of Colorado at Colorado
Springs, EAS#3, 1420,
Austin Bluffs Parkway,
Colorado Springs,
CO 80933-7150,
tboult@vast.uccs.edu,
and
Securics, Inc, Colorado Springs,
CO, USA

Kevin W. Bowyer
Department of Computer
Science and Engineering,
University of Notre Dame,
Notre Dame, IN, USA,
kwb@cse.nd.edu

Pradeep Buddharaju
Department of Computer Science,
University of Houston, 4800 Callhoun
Road, Houston, TX 77204, USA,
braju@cs.uh.edu

Paul W. Butler
Lumidigm, Inc.,
801 University Blvd. SE,
Suite 302,
Albuquerque, NM 87106, USA,
pbutler@lumidigm.com

Rama Chellappa
Center for Automation Research,
and Department of Electrical
and Computer Engineering,
University of Maryland,
College Park, MD 20742, USA,
rama@cfar.umd.edu

Sigmund Clausen
Idex ASA, Snarøya,
Norway,
sc@idex.no

Farzin Deravi
Department of Electronics,
University of Kent, UK,
F.Deravi@kent.ac.uk

Luca Didaci
Department of Electrical
and Electronic Engineering,
University of Cagliari Piazza d'Armi,
I-09123 Cagliari, Italy,
luca.didaci@diee.unica.it

Luciana Ferrer
Department of
Electrical Engineering,
Stanford University, CA, USA,
lferrer@speech.sri.com

Julian Fierrez
ATVS–Biometric Recognition Group,
Escuela Politecnica Superior,
Universidad Autonoma de Madrid,
Spain,
julian.fierrez@uam.es

Martin Fischler
SRI International,
333 Ravenswood Avenue,
Menlo Park, CA 94025, USA,
martin.fischler@sri.com

Patrick J. Flynn
Department of Computer
Science and Engineering,
University of Notre Dame,
Notre Dame, IN, USA,
flynn@cse.nd.edu

Annalisa Franco
C.d.L. Scienze dell'Informazione,
University of Bologna,
Via Sacchi 3, Cesena,
Italy,
annalisa.franco@unibo.it

Marc Friedman
Retica Systems Inc, Waltham,
Massachusetts, USA,
mfriedman@retica.com

Mitsutoshi Himaga
R&D Division, Hitachi-Omron
Terminal Solutions, Corp.,
Owari-asahi, Aichi, Japan,
mitsutoshi_himaga@hitachi-omron-ts.com

Sachin S. Kajarekar
SRI International,
Menlo Park, CA, USA,
sachin.kajarekar@sri.com

Katsuhiro Kou
Automated Teller Machine Systems
Group, Hitachi-Omron Terminal
Solutions, Corp., Shinagawa-ku,
Tokyo, Japan,
katsuhiro_kou@hitachi-omron-ts.com

B. V. K. Vijaya Kumar
Department of Electrical
and Computer Engineering,
Carnegie Mellon University,
Pittsburgh, Pennsylvania, USA,
kumar@ece.cmu.edu

Sang-Woong Lee
Korea University, Anam-dong
Seongbuk-ku, Seoul 136-713, Korea,
sangwlee@image.korea.ac.kr

Seong-Whan Lee
Korea University, Anam-dong
Seongbuk-ku, Seoul 136-713, Korea,
swlee@image.korea.ac.kr

Davide Maltoni
Scienze dell'Informazione,
Universitá di Bologna,
Via Sacchi 3, 47023
Cesena (FO), Italy,
davide.maltoni@unibo.it

Chinmay Manohar
Department of Internal Medicine,
Endocrine Research Unit,
Division of Endocrinology,
Mayo Clinic, Rochester,
MN 55905, USA,
manohar.chinmay@mayo.edu

Gian Luca Marcialis
Department of Electrical
and Electronic Engineering,
University of Cagliari Piazza d'Armi,
I-09123 Cagliari, Italy,
marcialis@diee.unica.it

James R. Matey
Sarnoff Corporation,
Princeton, NJ 08543-5300, USA,
jmatey@sarnoff.com

Gregory Myers
SRI International, 333 Ravenswood
Avenue, Menlo Park,
CA 94025, USA,
gregory.myers@sri.com

Jiří Navrátil
Conversational Biometrics Group,
IBM T.J. Watson Research Center,
1101 Kitchawan Road, Yorktown
Heights, NY 10598, USA,
jiri@us.ibm.com

Kristin Adair Nixon
Lumidigm, Inc.,
Suite 302,
801 University Blvd. SE,
Albuquerque, NM 87106, USA,
kanixon@lumidigm.com

Javier Ortega-Garcia
ATVS–Biometric Recognition Group,
Escuela Politecnica Superior,
Universidad Autonoma de Madrid,
Spain,
javier.ortega@uam.es

Geppy Parziale
Cogent Systems, Inc.,
South Pasadena, CA, USA,
gparziale@cogentsystems.com

Ioannis Pavlidis
Department of Computer Science,
University of Houston, 4800 Callhoun
Road, Houston, TX 77204, USA,
ipavlidi@central.uh.edu

Jason Pelecanos
Conversational Biometrics
Group, IBM T.J. Watson Research
Center, 1101 Kitchawan Road,
Yorktown Heights, NY 10598, USA,
jwpeleca@us.ibm.com

Ganesh N. Ramaswamy
Conversational Biometrics Group,
IBM T.J. Watson Research Center,
1101 Kitchawan Road,
Yorktown Heights, NY 10598, USA,
ganeshr@us.ibm.com

Fabio Roli
Department of Electrical
and Electronic Engineering,
University of Cagliari Piazza d'Armi,
I-09123 Cagliari, Italy,
roli@diee.unica.it

Robert K. Rowe
Lumidigm, Inc.,
Suite 302,
801 University Blvd. SE,
Albuquerque, NM 87106, USA,
rkrowe@lumidigm.com

Marios Savvides
Department of Electrical
and Computer Engineering,
Carnegie Mellon University,
Pittsburgh, Pennsylvania, USA,
Marios.Savvides@ri.cmu.edu

John K. Schneider
Ultra-Scan Corporation,
Amherst, New York, USA,
jschneider@ultra-scan.com

Lambert Schomaker
Department of Artificial Intelligence,
University of Groningen,
Grote Kruisstr. 2/1, 9712 TS,
Groningen, The Netherlands,
schomaker@ai.rug.nl

Elizabeth Shriberg
International Computer
Science Institute,
Berkeley, CA, USA,
elizabeth.shriberg@sri.com

Andreas Stolcke
SRI International,
Menlo Park,
and
International Computer
Science Institute,
Berkeley, CA, USA,
andreas.stolcke@sri.com

Deborah Thomas
Department of Computer
Science and Engineering,
University of Notre Dame,
Notre Dame, IN, USA,
dthomas4@cse.nd.edu

Jason Thornton
Department of Electrical
and Computer Engineering,
Carnegie Mellon University,
Pittsburgh, Pennsylvania, USA,
jthronto@andrews.cmu.edu

Michael Tinker
Sarnoff Corporation,
Princeton, NJ 08543-5300, USA,
mtinker@sarnoff.com

Yasunari Tosa
Retica Systems Inc.,
Waltham, Massachusetts, USA,
ytosa@retica.com

David Usher
Retica Systems Inc.,
Waltham, Massachusetts, USA,
dusher@retica.com

Masaki Watanabe
Fujitsu Laboratories Ltd.,
Kawasaki, Japan,
fabio-spr2007@ml.labs.fujitsu.com

Robert Woodworth
Securics, Inc., Colorado Springs,
CO, USA,
rwoodworth@securics.com

Chunyan Xie
Department of Electrical
and Computer Engineering,
Carnegie Mellon University,
Pittsburgh, PA, USA,
chunyanx@andrew.cmu.edu

Introduction

This book has 24 chapters and is divided into three parts: sensors, algorithms, and systems. There are nine chapters on sensors covering a wide range of traditional to novel data acquisition mechanisms, ten chapters on advanced algorithms for matching, and five chapters on system-level aspects such as standards and smartcards.

Part I: Sensors

Research has shown that biometric image quality is one of the most significant variables affecting biometric system accuracy and performance. We have included four chapters on the latest developments in fingerprint sensors covering multispectral imaging, touchless sensors, swipe sensors, and ultrasound capture. The chapter on multispectral imaging describes the capture of both the surface and subsurface features of the skin in order to generate a composite fingerprint image that has the added advantage of confirming "liveness" of human skin. The chapter on touchless fingerprint sensing presents a new approach that does not deform the skin during the capture, thus ensuring repeatability of measurements. The advantages and disadvantages with respect to legacy technology are highlighted. The chapter on swipe sensors is essentially about an image reconstruction algorithm that accounts for varying swiping speeds and directions. Finally, the chapter on ultrasonic imaging for livescan fingerprint applications describes how it is more tolerant to humidity, extreme temperatures, and ambient light when compared to optical scanners.

Measurement of vascular structures has been gaining popularity in mission-critical applications such as financial transactions because of the accuracy rendered and, more importantly, because of their robustness against spoof attacks. Two chapters on this topic have been included to provide an insight into this novel biometrics, both at the palm level as well as the finger level. The chapter on iris recognition systems describes image capture from moving subjects and at greater distances than have been available in the COTS.

The retina and iris are occular biometrics with uncorrelated complementary information and anatomical proximity allowing simultaneous capture by a single device. We have included a chapter that describes their integration into a single biometric solution. The final chapter in the sensors section is on the use of the facial vascular network, how it is highly characteristic of the individual, and how it can be unobtrusively captured through thermal imaging. The efficacy of this information for identity recognition is demonstrated by testing on substantial databases.

Part II: Algorithms

This part has two chapters pertaining to voice, two chapters that relate to handwriting, three chapters on face, and a chapter each on iris and headprint.

The first chapter on voice biometrics describes the general framework of a text-independent speaker verification system. It extracts short-term spectral features that implicitly capture the anatomy of the vocal apparatus and are complementary to spectral acoustic features. The other voice-related chapter introduces conversational biometrics, which is the combination of acoustic voice matching (traditional speaker verification) with other conversation-related information sources (such as knowledge) to perform identity verification.

The chapters on handwriting are on signature verification and writer identification. Readers will find the evaluation experiments to be an extremely useful benchmark in signature verification. The chapter reports results on a subcorpus of the MCYT biometric database comprising more than 7000 signatures from 145 subjects with comparisons to results reported at the First International Signature Verification Competition (SVC, 2004). The chapter on writer identification describes a methodology of combining textural, allographic, and placement features to improve accuracy.

The chapter on iris recognition asserts that matching performance becomes more robust when images are aligned with a flexible deformation model, using distortion-tolerant similarity cues. Again, useful benchmarks are provided by comparisons to the standard iris matching algorithm on the NIST Iris Challenge Evaluation (ICE, 2006).

Headprint-based recognition is a novel and unobtrusive biometric that is particularly useful in surveillance applications. The chapter presents new algorithms for separation of hair area from the background in overhead imagery and extraction of novel features that characterize the color and texture of hair. The more traditional biometrics used in surveillance are face and gait. However, current algorithms perform poorly when illumination conditions and pose are changing. We have therefore included one chapter that focuses on uncontrolled realistic scenarios, and another that proposes a new method of extending SVDD (Support Vector Data Description) to deal with noisy and degraded frames in surveillance videos. Face recognition from video also allows the use of multiple images available per subject. This strategy is described in a chapter where the emphasis is on selection of frames from the video sequences based on quality and difference from each other. Four different approaches have been compared on a video dataset collected by the University of Notre Dame. The last chapter on face biometrics deals with matching against large populations in real-time. This chapter introduces correlation pattern-recognition-based algorithms for the purpose.

Part III: Systems

There are five chapters in this part dealing with smartcards, privacy and security issues, methods for system-level improvements, and standards.

It has often been believed that the features derived from a biometric signal are not helpful in getting much information about the original biometrics and have been thought of loosely as a one-way hash of the biometrics. The chapter on fingerprint image synthesis disproves this notion by reconstructing the fingerprint image from its well-known industry standard template often used as a basis for information interchange between algorithms from multiple vendors. The results shown should convince the reader that the templates can be used to attack a biometrics system with these reconstructed images. A related advance covered in this chapter deals with detecting fake fingers based on odor sensing.

Whether it is a large-scale database such as US-VISIT or a small bank of biometrics stored on a server for logical access in an office, the solutions are based on insecure networks that are vulnerable to cyberattacks. The chapter on smartcards describes technology that eliminates the need for the database by both storing and processing biometric data directly on the card, thus providing security, privacy, dynamic flexibility, and scalability. Security and privacy are also the focus of the chapter on Biotopes™, which is essentially a method to transform the original biometric signature into an alternative revocable form (the Biotope) that protects privacy while supporting a robust distance metric necessary for approximate matching.

The chapter on adaptive biometric systems describes a method of improving performance by training on the fly. The unlabelled data that a system examines in test scenarios can be analyzed for parameters such as image quality (as they are sensor- and session-dependent), which can in turn be used adaptively by the recognition algorithms.

The final chapter of the book addresses the history, current status, and future developments of standardization efforts in the field of biometrics. The focus is on the activities of ISO's SC37 subcommittee dealing with biometric standardization.

References

SVC: http://www.cs.ust.hk/svc2004/
ICE: http://iris.nist.gov/ICE/

Part I

Sensors

1

Multispectral Fingerprint Image Acquisition

Robert K. Rowe, Kristin Adair Nixon, and Paul W. Butler

Abstract. This chapter describes the principles of operation of a new class of fingerprint sensor based on multispectral imaging (MSI). The MSI sensor captures multiple images of the finger under different illumination conditions that include different wavelengths, different illumination orientations, and different polarization conditions. The resulting data contain information about both the surface and subsurface features of the skin. These data can be processed to generate a single composite fingerprint image equivalent to that produced by a conventional fingerprint reader, but with improved performance characteristics. In particular, the MSI imaging sensor is able to collect usable biometric images in conditions where other conventional sensors fail such as when topical contaminants, moisture, and bright ambient lights are present or there is poor contact between the finger and sensor. Furthermore, the MSI data can be processed to ensure that the measured optical characteristics match those of living human skin, providing a strong means to protect against attempts to spoof the sensor.

1.1 Introduction

Biometric systems are deployed in order to provide a means of fixing the identity of individuals in an automated manner. In order for such a deployment to be successful, the biometric sensor needs to be able to collect useful data over the entire range of conditions in which it operates. These conditions include differences between users as well as variations in the environment in which the biometric measurement is taken. In addition, a biometric system should also be able to detect attempts to defeat it using some type of artificial sample without compromising successful use by a genuine authorized person. All of these capabilities should be able to be performed quickly and without extra steps or inconvenience to the authorized user.

Fingerprint sensing is one of the most widely deployed of all biometric technologies. There are a number of different techniques for capturing a fingerprint image including optical, capacitive, radio frequency, ultrasound, and thermal methods. One common shortcoming of many conventional fingerprint-sensing technologies is the frequent occurrence of poor-quality images under a variety of common operational circumstances. Although each particular imaging method has different sensitivities, in general poor images may result from conditions such as dry skin, worn surface features of the finger, poor contact between the finger and sensor, bright ambient light, and moisture on the sensor.

Many imaging technologies are also unable to provide strong affirmation that the fingerprint image is collected from a living unadulterated finger rather than an artificial or spoof sample. This is because the raw data collected by these systems contain little or no information about the physical properties of the fingerprint ridges presented. For example, a conventional optical fingerprint reader based on total internal reflectance (TIR) acquires images that represent the points of optical contact between the sensor platen and any material with a minimum index of refraction. Because many materials have an appropriate refractive index and can be formed to contain a fingerprint pattern, such a system is susceptible to spoof attempts.

To address these shortcomings, an optical fingerprint sensor has been developed that is able to work across the range of common operational conditions while also providing strong spoof detection. The sensor is based on multispectral imaging (MSI) and is configured to image both the surface and subsurface characteristics of the finger under a variety of optical conditions. The combination of surface and subsurface imaging ensures that usable biometric data can be taken across a wide range of environmental and physiological conditions. Bright ambient lighting, wetness, poor contact between the finger and sensor, dry skin, and various topical contaminants present little impediment to collecting usable MSI data.

A customized algorithm is used to fuse multiple raw MSI images into a single high-quality composite fingerprint image. This single fingerprint image can be used to match other MSI fingerprint images as well as images collected using other methods. Thus, the MSI fingerprint is backward compatible and can be used with existing fingerprint databases collected with different imaging technologies.

The surface and subsurface data collected by the MSI sensor provide rich information about the optical properties of the bulk sample. A classification methodology has been developed to operate on the MSI data and determine if the measured optical properties of the sample are consistent with those of living human skin. If so, the sample is deemed to be genuine; otherwise, the sample is identified as a possible spoof attempt. This provides the means by which an MSI sensor can provide strong assurance of sample authenticity.

This chapter describes the principles of operation of an MSI fingerprint sensor and illustrates the type of raw data that is collected. The methods used for generating a composite fingerprint are described and examples given. Medium-scale biometric performance testing procedures and results using these composite fingerprint images are provided. In a later section of this chapter, procedures and results from a study conducted under a variety of adverse conditions are presented. This study includes both an MSI fingerprint sensor as well as three common commercially available optical fingerprint sensors. Data from the same study are also analyzed in a way that demonstrates the cross-compatibility of MSI fingerprint images with those collected from conventional imagers. The final section of this chapter discusses MSI spoof detection methods and quantifies spoof detection performance.

1.2 Finger Skin Histology

Human skin is a complex organ that forms the interface between the person and the outside environment. The skin contains receptors for the nervous system, blood vessels to nourish the cells, sweat glands to aid thermal regulation, sebaceous glands for oil secretion, hair follicles, and many other physiologically important elements. As well, the skin itself is not a single homogeneous layer, but is made of different layers with different material properties. These different layers can be broadly separated into the epidermis, which is the most superficial layer, the dermis, which is the blood-bearing layer, and the subcutaneous skin layer which contains fat and other relatively inert components.

The skin on the palmar side of the finger tips contains dermatoglyphic patterns comprising the ridges and valleys commonly measured for fingerprint-based biometrics. It is important to note that these patterns do not exist solely on the surface of the skin: many of the anatomical structures below the surface of the skin mimic the surface patterns. For example, the interface between the epidermal and dermal layers of skin is an undulating layer made of multiple protrusions of the dermis into the epidermis known as dermal papillae. These papillae follow the shape of the surface dermatoglyphic patterns (Cummins and Midlo, 1961) and thus represent an internal fingerprint in the same form as the external pattern. Small blood vessels known as capillaries protrude into the dermal papillae (Sangiorgi et al., 2004) as shown in Figure 1.1. These blood vessels form another representation of the external fingerprint pattern.

There are various methods that can be used to image the internal structure of the skin of the finger. One method is the use of optics. Recently published research demonstrated the use of optical coherence tomography to investigate features of the finger skin below the ridges and valleys (Shirastsuki et al., 2005). This research showed that there was a distinct area of high reflectivity (at 850 nm) in the skin approximately 500 μm below each finger ridge. Furthermore, the researchers were able to demonstrate that this subsurface pattern continued to exist even when the surface pattern was deformed by application of high pressure or obscured by a wrinkle in the skin.

Multispectral imaging represents another optical method that can be used to capture surface and subsurface features of the skin. The remainder of this chapter provides details on MSI operational principles as well as tests and results from this type of fingerprint sensor.

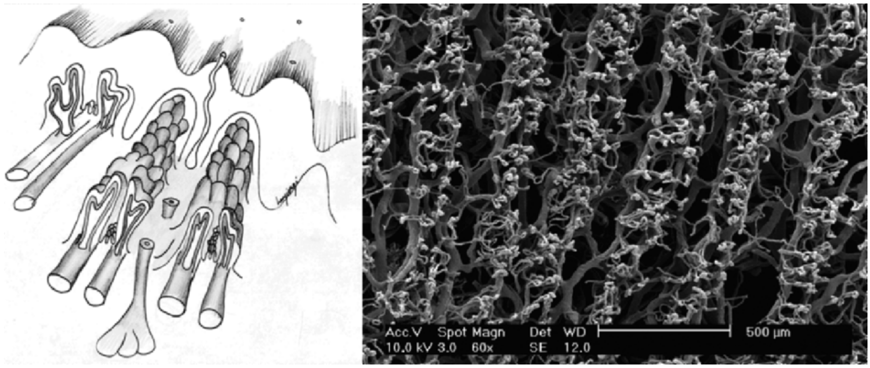

Fig. 1.1. Histology of the skin on the palmar surface of the fingertip. The sketch on the left shows the pattern of the capillary tufts and dermal papillae that lie below the fingerprint ridges. The SEM photo on the right side shows the rows of capillary tufts imaged on a portion of an excised thumb after the surrounding skin has been removed (Simone Sangiorgi, personal communication, 2005).

1.3 MSI Principles of Operation

In order to capture information-rich data about the surface and subsurface features of the skin of the finger, the MSI sensor collects multiple images of the finger under a variety of optical conditions. The raw images are captured using different wavelengths of illumination light, different polarization conditions, and different illumination orientations. In this manner, each of the raw images contains somewhat different and complementary information about the finger. The different wavelengths penetrate the skin to different depths and are absorbed and scattered differently by various chemical components and structures in the skin. The different polarization conditions change the degree of contribution of surface and subsurface features to the raw image. Finally, different illumination orientations change the location and degree to which surface features are accentuated.

Figure 1.2 shows a simplified schematic of the major optical components of an MSI fingerprint sensor. Illumination for each of the multiple raw images is generated by one of the light emitting diodes (LEDs). The figure illustrates the case of polarized direct illumination being used to collect a raw image. The light from the LED passes through a linear polarizer before illuminating the finger as it rests on the sensor platen. Light interacts with the finger and a portion of the light is directed toward the imager through the imaging polarizer. The imaging polarizer is oriented with its optical axis to be orthogonal to the axis of the illumination polarizer, such that light with the same polarization as the illumination light is substantially attenuated by the polarizer. This severely reduces the influence of light reflected from the surface of the skin and emphasizes light that has undergone multiple optical scattering events after penetrating the skin.

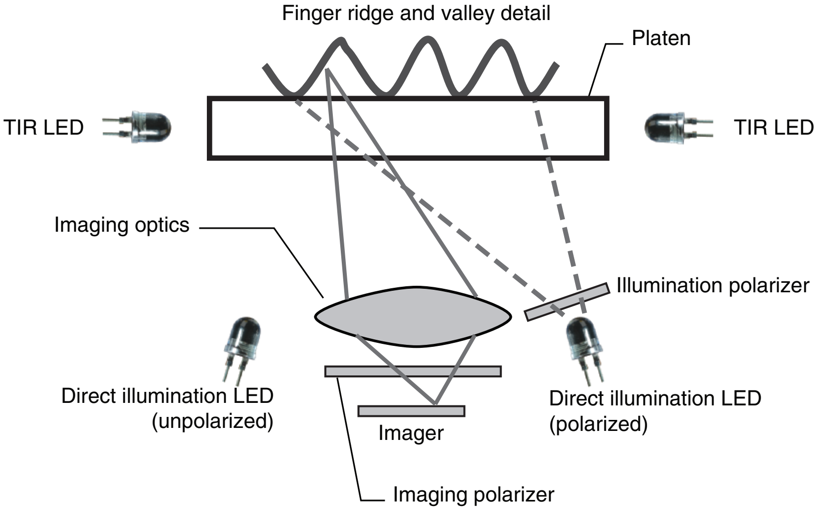

Fig. 1.2. Optical configuration of an MSI sensor. The dotted lines illustrate the direct illumination of a finger by a polarized LED.

The second direct illumination LED shown in Figure 1.2 does not have a polarizer placed in the illumination path. When this LED is illuminated, the illumination light is randomly polarized. In this case the surface-reflected light and the deeply penetrating light are both able to pass through the imaging polarizer in equal proportions. As such, the image produced from this non-polarized LED contains a much stronger influence from surface features of the finger.

It is important to note that all of these direct illumination sources (both polarized and nonpolarized) as well as the imaging system are arranged to avoid any critical-angle phenomena at the platen–air interfaces. In this way, each illuminator is certain to illuminate the finger and the imager is certain to image the finger regardless of whether the skin is dry, dirty, or even in contact with the sensor. This aspect of the MSI imager is distinctly different from most other conventional fingerprint imaging technologies and is a key aspect of the robustness of the MSI methodology.

In addition to the direct illumination illustrated in Figure 1.2, the MSI sensor also integrates a form of TIR imaging, illustrated in Figure 1.3. In this illumination mode, one or more LEDs illuminates the side of the platen. A portion of the illumination light propagates through the platen by making multiple TIR reflections at the platen–air interfaces. At points where the TIR is broken by contact with the skin, light enters the skin and is diffusely reflected. A portion of this diffusely reflected light is directed toward the imaging system and passes through the imaging polarizer (because this light is randomly polarized), forming an image for this illumination state. Unlike all of the direct illumination states, the quality of the resulting raw TIR image is critically

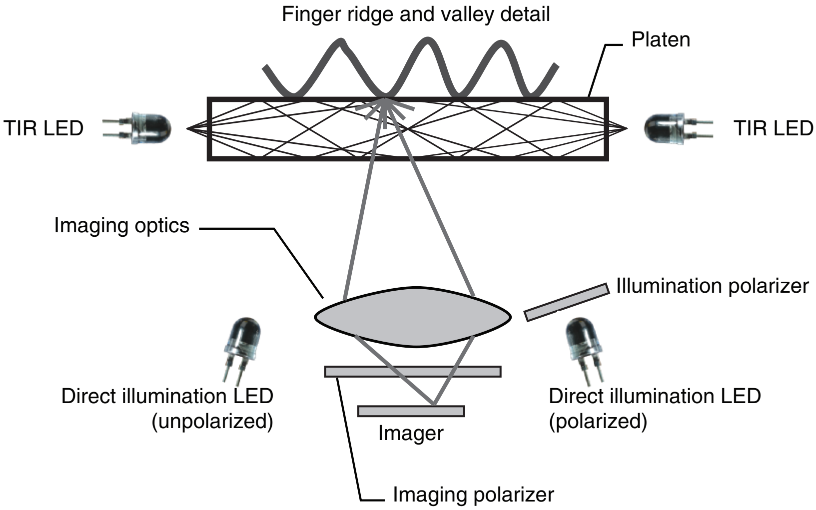

Fig. 1.3. MSI sensor schematic showing TIR illumination.

dependent on having skin of sufficient moisture content and cleanliness making good optical contact with the platen, just as is the case with conventional TIR sensors. However, unlike conventional TIR sensors, the MSI sensor is able to form a usable representation of the fingerprint from the direct illumination images even when the TIR image is degraded or missing. Further details of this are provided in later sections of this chapter.

In practice, MSI sensors typically contain multiple direct-illumination LEDs of different wavelengths. For example, the Lumidigm J110 MSI sensor shown in Figure 1.4 is an industrial-grade sensor that has four direct-illumination wavelength bands (430, 530, and 630 nm as well as a white light) in both polarized and unpolarized configurations. When a finger is placed on the sensor platen, eight direct-illumination images are captured along with a single TIR image. The raw images are captured on a 640×480 image array with a pixel resolution of 525 ppi. All nine images are captured in approximately 500 mSec.

In addition to the optical system, the sensor shown in Figure 1.4 comprises control electronics for the imager and illumination components, an embedded processor, memory, power conversion electronics, and interface circuitry. The embedded processor performs the image-capture sequence and communicates to the rest of the biometric system through the interface circuitry. In addition to controlling the image acquisition process and communications, the embedded processor is capable of processing the nine raw images to generate a single 8-bit composite fingerprint image from the raw data. The embedded processor also analyzes the raw MSI data to ensure that the sample being imaged is a genuine human finger rather than an artificial or spoof material. Composite fingerprint image generation and spoof detection are described in

Fig. 1.4. Lumidigm J110 industrial MSI fingerprint sensor with embedded processing capable of performing autonomous generation of a composite fingerprint image, spoof detection, feature extraction, matching, and network communications.

greater detail in the following sections. In some applications, the J110 is also configured to perform onboard feature extraction and matching.

1.4 Composite Fingerprint Image Generation

As described in the previous section, multiple raw images of the finger are collected each time a finger touches the sensor. These multiple images correspond to different illumination wavelengths, polarization conditions, and optical geometries. As such, each contains a slightly different representation of the characteristics of the finger, including the fingerprint itself. An example of the raw images derived during a single measurement from a Lumidigm J110 MSI sensor is shown in Figure 1.5. The upper row shows the raw images for unpolarized illumination wavelengths of 430, 530, and 630 nm, as well as white light. The middle row shows the corresponding images for the cross-polarized case. The single image on the bottom row is the TIR image. The grayscale for each of the raw images has been expanded to emphasize the features.

It can be seen from the figure that there are a number of features present in the raw data including the textural characteristics of the subsurface skin, which appears as mottling that is particularly pronounced under blue (430 nm) and green (530 nm) illumination wavelengths. As well, the relative intensities of the raw images under each of the illumination conditions is very indicative of the spectral characteristics (i.e., color) of the finger or other sample (note

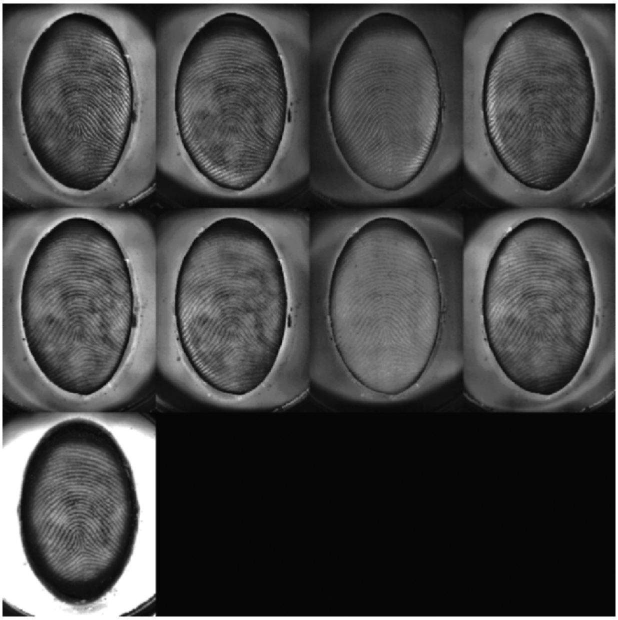

Fig. 1.5. Raw MSI images. The upper row of images corresponds to cross-polarized illumination of various wavelengths, the middle row corresponds to cross-polarized illumination, and the bottom left image is a backscattered image.

that the relative intensities have been obscured in Figure 1.5 to better show the comparative details of the raw images). Both textural and spectral characteristics play a key role in spoof detection because each exhibits distinct differences between living skin and most other materials. Methods of using these characteristics for spoof detection are more fully described in a later portion of this chapter.

Also of note in the raw images is the area of the finger that each captures. The directly illuminated images in the top and middle rows capture details over nearly the entire surface of the finger. In contrast, the TIR image in the bottom row only captures features from a smaller central portion of the finger, as evinced by the size of the illuminated region in the image. This difference is due to the fact that the TIR image requires optical contact between the finger and platen to generate an image whereas direct illumination does not require contact and can thus effectively capture features of the finger even in those areas where there is a gap between the skin and the platen. This is significant because the MSI images contain information about the finger over a bigger area than an equivalent surface-based imaging technology is capable of capturing, which would be expected to result in additional biometric features (e.g., minutiae) and a corresponding improvement in biometric performance.

Fig. 1.6. On the left is a composite fingerprint image generated from the raw MSI images shown in Figure 1.5. On the right is a conventional TIR image collected on the same finger used to generate the MSI fingerprint.

The set of raw images shown in Figure 1.5 can be combined to produce a single representation of the fingerprint pattern. This fingerprint generation relies on a wavelet-based method of image fusion to extract, combine, and enhance those features that are characteristic of a fingerprint. The wavelet decomposition method that is used is based on the dual-tree complex wavelet transform (Kingsbury, 2001). Image fusion occurs by selecting the coefficients with the maximum absolute magnitude in the image at each position and decomposition level (Hill et al., 2002). An inverse wavelet transform is then performed on the resulting collection of coefficients, yielding a single composite image. An example of the result of applying the compositing algorithm to the raw data in Figure 1.5 is shown in Figure 1.6. Fine structure such as incipient fingerprint ridges can be seen throughout the image. For comparison, a conventional (TIR) fingerprint image was collected on the same finger and is also shown.

1.5 Biometric Testing and Results

1.5.1 Baseline Performance

The baseline performance of the J110 MSI sensor was assessed in a recent multi-person study. Three Lumidigm J110 sensors were deployed in the study in which 118 people were recruited to participate. The study duration was three weeks long, during which time the volunteers made multiple visits. Volunteers were divided roughly evenly between males and females. The ages ranged between 18 and over 80 years old. Volunteers were not prescreened for any particular characteristic and the demographic distribution of the volunteers participating in the study generally reflected the local (Albuquerque, New Mexico) population.

All fingers (i.e., index, middle, ring, and little finger) of the right hand of each volunteer were measured at multiple times throughout the study. The first three presentations of a particular finger on the first J110 sensor were used as enrollment data against which data taken on all other sensors and during subsequent visits were compared. Volunteers came "as they were" to each study session and were not asked to wash their hands or pretreat the finger skin in any way.

The biometric performance was assessed using a feature extraction and matching algorithm supplied by NEC (NECSAM FE4, ver. 1.0.2.0, PPC2003). The match values were generated by comparing each of the verification templates against each of the three enrollment templates and the highest match value was taken. All properly labeled images were used for the analysis of biometric performances. The only images that were omitted from analysis were a small number that were collected on incorrect fingers. These occurrences were assessed using Web cameras and other supplemental means and were not based on the fingerprint match itself.

The receiver operating characteristic (ROC) curve generated from the study is shown in Figure 1.7. The equal error rate (EER) is approximately 0.8% and the false rejection rate (FRR) at a false acceptance rate (FAR) of 0.01% is approximately 2.5%, corresponding to a true acceptance rate (TAR) of 97.5%. The total number of true-match comparisons used for this curve is 5811 and the number of false-match comparisons is 58,110, randomly chosen from all possible false-match comparisons.

1.5.2 Comparative Performance Under Adverse Influences

The hypothesis that the MSI sensor has the ability to collect usable biometric data under conditions where the performance of other sensors degrades or the sensor stops working was tested in a series of comparative multiperson studies. The studies included both an MSI sensor as well as several conventional TIR fingerprint sensors. In order to draw a strong conclusion from the study and avoid spurious results, key aspects of the experiment were varied and the resulting findings were compiled to yield the overall conclusions. These key experimental aspects include the following.

- Conventional TIR sensor performance was assessed using three different commercially available TIR sensors from three different manufacturers.

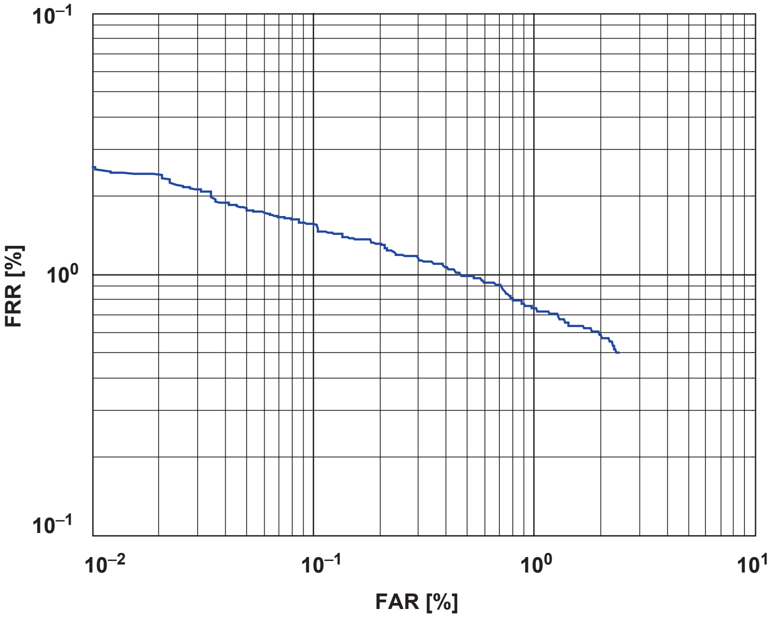

Fig. 1.7. Baseline biometric performance of the J110 MSI fingerprint sensor assessed during a three-week study of 118 volunteers using all four fingers (index, middle, ring, and little finger) of their right hand.

- Three different commercially available feature extractors and matchers were used to assess biometric performance across all images.
- Six different adverse conditions were tested.

In addition to the Lumidigm J110 MSI fingerprint sensor, the three conventional TIR sensors used in the study were:

- Cross Match Verifier 300 ("Sensor C")
- Identix DFR 2100 ("Sensor I")
- Sagem Morpho MSO 300 ("Sensor S")

The three commercially available fingerprint algorithms used to generate results from all images were from NEC, Sagem, and Neurotechnologija. The results presented below were generated by taking the average of the results produced by each of these algorithms.

The six different adverse conditions that were tested were as follows.

- Acetone: Approximately a teaspoon of acetone was poured on each finger and allowed to dry prior to the collection of each image.
- Chalk: The volunteer was asked to take a small pinch of chalk and rub it between his or her fingers prior to each image collection. The chalk was white climber's chalk obtained from a local sporting goods store.

- Dirt: The volunteer was asked to take a small pinch of dirt and rub it between his or her fingers prior to image collection. The dirt was collected locally and consisted of sand, small stones, humus, and the like.
- Water: Volunteers were asked to dip their fingers in a glass of water and immediately place the wet finger on the sensor prior to each image collection.
- Low pressure: The volunteer was asked to "barely touch" the sensor, resulting in an estimated force of 0.2–3.0 ounces.
- Bright ambient light: Three quartz tungsten halogen (QTH) lamps with a total wattage of 1100 W were placed at a height of approximately 30 in. and a fixed orientation relative to the platen of each sensor. This resulted in an incident intensity of approximately 7.35 K Lux on the platen surface when no finger was present.

The study of the effect of these adverse conditions was initiated by recruiting approximately 20 volunteers for each experimental session (not all volunteers were able to participate in all portions of the study) from the local office environment. Each volunteer enrolled four fingers (left middle, left index, right index, right middle) on each of the study sensors under benign indoor ambient conditions. Enrollment consisted of collecting three high-quality images of each finger during a supervised session. During the enrollment session, the expert supervisor examined each image prior to accepting it in order to ensure that the image was properly centered and contained good detail about the fingerprint pattern. In some cases a volunteer was asked to place a small amount of skin lotion on his or her fingertips in order to obtain an image of sufficient quality from one or more of the conventional TIR sensors.

On subsequent test days, the volunteers presented themselves at the measurement station and images would be taken of each of the enrolled fingers under the designated adverse condition for the session. All of the sensors were tested during each session, in close succession, and under as similar conditions as possible. In some cases, one or more of the conventional TIR sensors experienced a failure to acquire (FTA) due to the real-time image acquisition logic incorporated in the sensor. In those cases where a volunteer was unable to successfully collect an image after approximately ten seconds, a blank image was inserted in its place and used in the subsequent analysis.

Each of the images in the resulting datasets was matched against each of the enrollment images. The highest match value across the three enrollment images was saved and accumulated to compile the matching and nonmatching values and resulting performance curves for each of the three feature-extraction and matching packages. The final results were generated by averaging the performance values for the three matchers.

The size of the dataset for each adverse condition was approximately 230 images, which was used to generate an equivalent number of true-match comparison values. The number of false-match comparisons used for each

Table 1.1. TAR (%) at an FAR of 0.01%. Sensor C is a Cross Match Verifier 300, Sensor I is an Identix DFR 2100, Sensor S is a Sagem MSO300, and the MSI Sensor is a Lumidigm J110.

	Sensor C	Sensor I	Sensor S	MSI Sensor
Acetone	62.9	97.0	82.8	99.1
Chalk	0.1	1.9	2.2	91.8
Dirt	0.5	7.8	4.3	85.9
Water	18.4	12.1	14.4	99.3
Low pressure	40.2	52.9	39.5	98.0
Bright ambient	5.5	48.8	99.3	99.8
Average (all conditions)	21.3	36.8	40.4	95.7

condition and algorithm varied between 5676 and 22,700 randomly selected from all possible false-match comparisons.

A table summarizing the resulting average biometric performance of each of the tested sensors under each adverse condition is given in Table 1.1. The table shows the TAR corresponding to an FAR = 0.01%.

The performance of the MSI sensor can be seen to be significantly better than the conventional sensors in both the average case and in most specific instances. In some cases, the performance difference is quite dramatic (e.g., the case of water on the platen). This performance difference is generally maintained at all operating points along the respective ROC curves.

1.5.3 Backward Compatibility with Legacy Data

The enrollment and verification data collected with the four different sensors and the six different adverse conditions were analyzed a second way to assess the ability of the MSI images to be matched to images collected from conventional TIR fingerprint sensors. To make this assessment, the MSI images that were collected under the adverse conditions were matched to the enrollment data collected from each of the conventional TIR sensors. As before, the analysis was repeated for each of the three extractor–matcher software packages. Table 1.2 summarizes the resulting average performance results.

Same-sensor performance, repeated from Table 1.1, corresponds to cross-sensor matching results. A comparison of the cross-sensor and same-sensor results shows a dramatic improvement in nearly every tested instance as well as the overall average. This finding indicates that the MSI imaging technology is compatible with legacy data collected on conventional TIR fingerprint sensors. Moreover, the performance improvements of the MSI sensor operating in adverse conditions can be realized even in cases where the enrollment data are taken under a different imaging method. This is consistent with the premise that an MSI imager can acquire raw data sufficient to produce a high-quality composite fingerprint image under conditions where other technologies experience severe performance degradation.